

000 SYMBOLIC OR NUMERICAL? 001 002 UNDERSTANDING PHYSICS PROBLEM SOLVING IN REA- 003 SONING LLMs 004

005
006 **Anonymous authors**
007 Paper under double-blind review
008
009
010

011 ABSTRACT 012

013 Navigating the complexities of physics reasoning has long been a difficult task for
014 Large Language Models (LLMs), requiring a synthesis of profound conceptual un-
015 derstanding and adept problem-solving techniques. In this study, we investigate the
016 application of advanced instruction-tuned reasoning models, such as Deepseek-R1,
017 to address a diverse spectrum of physics problems curated from the challenging
018 SciBench benchmark. Our comprehensive experimental evaluation reveals the
019 remarkable capabilities of reasoning models. Not only do they achieve state-of-
020 the-art accuracy in answering intricate physics questions, but they also generate
021 distinctive reasoning patterns that emphasize on symbolic derivation. Furthermore,
022 our findings indicate that even for these highly sophisticated reasoning models, the
023 strategic incorporation of few-shot prompting can still yield measurable improve-
024 ments in overall accuracy, highlighting the potential for continued performance
025 gains.

026 1 INTRODUCTION 027

028 Recent advances in large language models (LLMs), particularly models such as GPT-01 and
029 DEEPSEEK-R1, have substantially improved the capabilities of numerous complex reasoning tasks
030 OpenAI (2023); Chung et al. (2022). Historically, researchers have used a wide range of specialized
031 methods and sophisticated prompt engineering techniques, including chain-of-thought prompting Wei
032 et al. (2022), structured few shot prompting Brown et al. (2020), and retrieval-augmented generation
033 Lewis et al. (2020) to improve LLM performance in challenging domains such as physics.

034 Despite their success, these traditional approaches typically incur significant effort in the design of
035 domain-specific prompts and the maintenance of auxiliary systems. Moreover, the performance of
036 these approaches can vary widely depending on the effectiveness of prompt construction and the
037 availability of external computational tools Madaan et al. (2023); Huang et al. (2023). Consequently,
038 there is an ongoing demand to explore simpler yet equally effective strategies to leverage the inherent
039 reasoning capabilities of modern LLMs, particularly as these models continue to grow in size and
040 sophistication Kaplan et al. (2020).

041 The advent of advanced reasoning-focused models has raised important questions about the necessity
042 and efficiency of these complex engineering efforts. These recent models are specifically optimized
043 through extensive instruction tuning and reinforcement learning from human feedback Ouyang et al.
044 (2022); Taori et al. (2023), enhancing their native ability to reason logically and coherently without
045 relying heavily on external assistance. In this work, we empirically investigate whether contemporary
046 instruction-tuned reasoning models can independently achieve high performance on physics reasoning
047 tasks without extensive prompt engineering or external augmentation and what reasoning mechanisms
048 underlie their behavioral divergence from standard chat models. Additionally, we seek to determine
049 whether carefully designed few-shot prompt engineering continues to provide measurable benefits for
050 advanced LLMs in the physics domain.

051 We evaluate the DEEPSEEK-R1 and its distilled models across three representative physics datasets
052 from the SciBench benchmark Chen et al. (2023), covering fundamental topics such as classical
053 dynamics, thermodynamics, and fundamental physics and comprising diverse and challenging prob-
lems.

Our findings demonstrate that reasoning-focused LLMs alone attain satisfactory results, achieving competitive accuracy on challenging physics problems. Furthermore, we show that targeted few-shot prompts can still enhance the performance of advanced models, providing valuable improvements in accuracy and interpretability. Moreover, our study reveals distinctive reasoning patterns by analyzing the chain-of-thought (CoT) outputs generated by different types of models. We observe that reasoning-specialized models prefer symbolic derivation—algebraically manipulating equations before numeric substitution—to solve physics calculation problems in most cases, in contrast to chat-oriented models that rely on procedural, step-by-step numerical substitution. This divergence highlights symbolic reasoning as a distinguishing factor contributing to the accuracy and robustness of reasoning-specialized models in multi-step scientific problem-solving tasks.

2 RELATED WORK

2.1 PHYSICS PROBLEM SOLVING WITH LLMs

Early efforts to apply large language models (LLMs) to physics reasoning treated textbook-style questions as pure text-completion tasks. For example, Gao et al. Gao et al. (2022) evaluated GPT-3 on introductory mechanics and electromagnetism problems, finding limited success with zero-shot prompting, especially on multi-step derivations. To improve performance, Wei et al. Wei et al. (2022) introduced a prompt *chain-of-thought*, demonstrating substantial gains in math and logic benchmarks; subsequent work by Kojima et al. Kojima et al. (2022) extended these benefits to physics questions.

More recent approaches combine LLMs with external tools. Program-aided language models (Liu et al. Liu et al. (2023)) integrate symbolic solvers for arithmetic and algebraic steps, while tool-augmented frameworks (Huang et al. Huang et al. (2023)) call unit conversion libraries and equation solvers via APIs. Self-verification techniques (Nye et al. Nye et al. (2024)) further enhance reliability by having the model re-check its solution steps against physical laws. These methods, however, require additional infrastructure or fine-tuning. In contrast, our work examines the power of *in-context* prompt design alone—without external tools or parameter updates—to boost pure physics reasoning in state-of-the-art instruction-tuned models.

2.2 PROMPT ENGINEERING AND ADVANCED LANGUAGE MODELS

The paradigm of *few-shot prompting* was popularized by Brown et al. Brown et al. (2020), who showed that adding exemplars in the prompt can dramatically improve LLM performance. Based on this, the decomposition prompts (Madaan et al. Madaan et al. (2023)) explicitly break problems into sub-questions within the context. As LLMs have been refined through instruction tuning (Chung et al. Chung et al. (2022)), reinforcement learning from human feedback (Ouyang et al. Ouyang et al. (2022)) and specialized reasoning curricula (Smith et al. Smith et al. (2023)), the marginal gains from complex prompts have come under scrutiny.

Zheng et al. Zheng et al. (2024) evaluated prompt variants in GPT-4 code generation, finding that simple zero-shot prompts often matched or outperformed elaborate few-shot templates. Li et al. Li et al. (2024) similarly observed that instruction-tuned models can produce high-quality reasoning chains without exemplars on logic puzzles. However, these studies focus on general coding or reasoning benchmarks rather than domain-specific tasks. Our paper fills this gap by systematically studying few shot physics prompts in advanced reasoning models, demonstrating that carefully chosen exemplars continue to yield significant accuracy improvements in physics problem solving.

3 EXPERIMENT

3.1 OVERVIEW

Our experimental workflow, as Figure 1 illustrates, systematically assesses the problem-solving capabilities of reasoning-tuned LLMs on physics questions. We begin by selecting a representative set of problems from the SciBench Chen et al. (2023) benchmark, encompassing mechanics, thermodynamics, and electromagnetism, and formatting each into a standardized prompt. For every problem, we generate both a Zero-Shot CoT prompt and a Few-Shot CoT prompt. We then run these prompts

108 through our reasoning models and baseline chat models in parallel to compare their performance in
 109 terms of accuracy and error categories. During inference, we record the complete Chain-of-Thought
 110 outputs for both reasoning and chat models to evaluate not only the final answer but also the quality
 111 of their intermediate reasoning steps.
 112

113 **3.2 DATASETS**

116 We conduct experiments using three representative datasets from the SciBench benchmark. After
 117 filtering out problems that require detailed solutions and visual components, we focus exclusively on
 118 textbook-style questions. The resulting datasets are summarized in Table 1.
 119

120	Dataset	Field	# P	# S
121	fund	fundamental physics	71	10
122	thermo	thermodynamics	66	17
123	class	classical dynamics	56	7

125 Table 1: Dataset statistics after filtering out problems with visuals. #S denotes the number of available
 126 detailed solution per subset.
 127

129 **Dataset Selection.** We selected the dataset from SciBench due to its challenging nature: solving
 130 these problems requires not only scientific literacy but also strong reasoning skills, including complex
 131 calculations and step-by-step logical deduction. This effectively distinguishes model capabilities.
 132 Moreover, the dataset spans diverse fields and ranges from three different physics fields: electronics,
 133 thermodynamics, and classical dynamics.

134 **Dataset Filtering.** Since some baseline chat models lack multimodal capabilities, we exclude
 135 problems containing visual elements and focus solely on textual problems. Additionally, we filter out
 136 problems with detailed solutions to ensure they can be used as few-shot prompts.
 137

138 **3.3 MODELS**

140 **Selected Model.** In the experiment, we select Deepseek-R1 and its distilled models R1-distill-
 141 LLaMA-70B and R1-distill-Qwen-32B. They are highly efficient open-weight models designed to
 142 balance strong reasoning capabilities with reduced computational costs. DeepSeek-R1 demonstrates
 143 robust performance in complex reasoning tasks, while its distilled versions maintain competitive
 144 ability, leveraging knowledge transfer from larger teacher models (LLaMA-70B and Qwen-32B)
 145 to achieve cost efficiency. The distillation process optimizes inference speed and memory usage,
 146 allowing R1-distill variants to deliver cost-effective alternatives while retaining core logical and
 147 analytical strengths.

148 **Baselines.** We compare the results of our models against baseline performances reported in the
 149 SciBench benchmark Chen et al. (2023). SciBench evaluates the reasoning capabilities of a wide
 150 range of general-purpose large language models across various physics domains using a unified
 151 framework. The benchmark includes standard instruction-tuned models such as LLaMA-2 (7B and
 152 70B), MISTRAL-7B, CLAUDE2, GPT-3.5-TURBO, GPT-4, and GPT-4-TURBO, assessed under
 153 both zero-shot and few-shot Chain-of-Thought (CoT) prompting settings. In doing so, we aim to make
 154 a comprehensive comparison of the reasoning capability between reasoning models and chat-based
 155 models.

156 **Parameters Setup.** In our implementation, parameters are configured to ensure stable and repro-
 157 ducible model inference. We set the temperature to a near-zero value (1e-30) to eliminate sampling
 158 variability, thereby enforcing deterministic behavior and ensuring consistency across repeated runs.
 159 The number of returned completions is set to one (n=1), as our evaluation focuses on top-1 perfor-
 160 mance. To enhance robustness, the retry mechanism is configured with a high tolerance for failure:
 161 the patience parameter is set to 10^9 , allowing the system to persist through transient API issues
 without manual intervention.

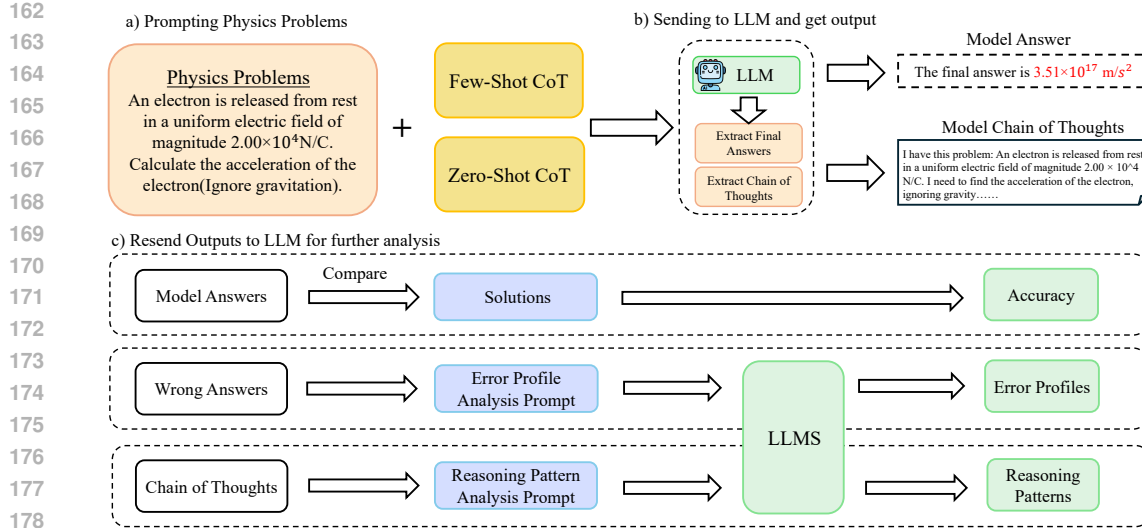


Figure 1: Overview of the experimental pipeline. A diverse set of physics problems is sampled from three domains: Fund, Thermo, and Class. Each problem is fed into the model under two prompting conditions: (1) Zero-shot Chain-of-Thought (CoT) prompting, and (2) Few-shot CoT. The model’s output solutions and CoT traces are evaluated along two axes by sending back to LLMs: error categorization (analyzing incorrect reasoning types) and reasoning pattern analysis (identifying characteristic cognitive strategies).

3.4 PROMPTING CONDITIONS

We test model performance under two distinct prompting strategies:

- **Zero-Shot CoT.** The model is prompted to “think step by step” before answering, but receives no prior examples. The goal is to test whether the instruction-tuned reasoning capabilities of DEEPSEEK-R1 are sufficient to generate coherent multi-step solutions without external exemplars.
- **Few-Shot CoT.** The prompt is prepended with a few example problems, drawn from existing dataset instances that include detailed solutions. For controlled experimentation, we select only the top three exemplars from each subset.

These strategies allow us to analyze not only the final accuracy, but also the structure and correctness of the intermediate reasoning steps, which is critical to understanding whether errors stem from flawed logic or mere computational missteps. The zero-shot approach highlights the model’s intrinsic reasoning capabilities, while the few-shot setting measures its ability to adapt to demonstrated solution patterns. This dual evaluation provides deeper insights into the model’s problem-solving robustness beyond surface-level metrics.

3.5 EVALUATION METHOD

Accuracy. The evaluation of the accuracy of the solution is carried out by comparing each numerical response generated by the model with the reference value within a fixed relative tolerance of 5%. A response is considered to be correct if its parsed value falls within the specified tolerance of the ground-truth answer.

Error Categories. To better understand the shortcomings in incorrect solutions, we analyzed error types using the *SciBench* error automatic categorization framework, which employs an LLM to verify incorrect solutions and classify the error type of each one. This allows us to identify key reasoning gaps and assess the strengths of different models.

Chain-of-thought Output. Chain-of-thought outputs from LLMs are collected by embedding three exemplar problem–solution pairs. The model’s subsequent output—which interleaves reasoning

Model	Zero-Shot + CoT Wei et al. (2022)				Few-Shot + CoT Wei et al. (2022)			
	Fund	Thermo	Class	Avg	Fund	Thermo	Class	Avg
LLaMA-2-7B	0.00%	0.00%	0.67%	0.22%	1.87%	5.48%	3.60%	3.65%
LLaMA-2-70B	0.93%	0.00%	1.89%	0.94%	13.10%	12.33%	8.40%	11.28%
Mistral-7B	6.54%	0.00%	4.63%	3.72%	6.54%	2.13%	6.09%	4.92%
Claude2	20.56%	3.08%	10.99%	11.54%	15.89%	6.12%	15.26%	12.42%
GPT-3.5-Turbo	6.54%	10.20%	12.19%	9.64%	8.41%	6.12%	11.99%	8.84%
GPT-4	28.04%	20.41%	25.37%	24.61%	41.12%	16.33%	25.36%	27.60%
GPT-4-Turbo	60.75%	28.57%	42.37%	43.90%	59.81%	18.37%	39.45%	39.21%
Deepseek-V3	63.40%	50.00%	65.20%	59.53%	53.50%	32.10%	25.80%	37.13%
R1-distill-LLaMA-70B	64.80%	55.40%	68.20%	62.80%	62.00%	50.00%	<u>66.70%</u>	59.57%
R1-distill-Qwen-32B	<u>76.10%</u>	<u>74.50%</u>	66.70%	<u>72.43%</u>	<u>74.60%</u>	<u>65.20%</u>	51.80%	<u>63.87%</u>
Deepseek-R1	88.70%	76.50%	62.50%	75.90%	93.00%	66.10%	84.80%	81.30%

Table 2: Physics accuracy (%) on the *fund*, *thermo*, and *class* domains under Zero-Shot and Few-Shot CoT prompting for models ranging from LLaMA-2-7B through GPT-4-Turbo. **Bold** indicates the best result per column; underline, the second-best. Model performance data from LLaMA-2-7B through GPT-4-Turbo is drawn from the SciBench benchmark. Chen et al. (2023).

steps with the final boxed answer—is recorded in full for each instance. Downstream analysis then proceeds by closely examining representative correct and incorrect reasoning chains to identify systematic inferential faults and reasoning patterns. This process involves human reviewers analyzing the CoT outputs to discern distinct reasoning patterns, and subsequently designing prompts that guide LLMs to analyze solutions for classification of reasoning patterns.

4 RESULTS

4.1 PERFORMANCE ACROSS DATASETS

Comparison to Baseline Models. Compared to general-purpose models like GPT-4, Claude2, and GPT-3.5-Turbo, the R1-series models (Deepseek-R1 and its distilled versions) show a clear advantage in physics-related tasks. For instance, in zero-shot mode, Deepseek-R1’s average accuracy (75.9%) was nearly double that of GPT-4-Turbo (43.9%), with particularly large gaps in Fund (88.7% vs. 60.75%). The distilled models maintained competitive performance while potentially offering better computational efficiency, suggesting that model distillation can retain high accuracy while reducing resource demands.

Impact of Few-Shot Prompting. Our experiments reveal that few-shot prompting continues to offer tangible benefits, even for models that already exhibit strong zero-shot reasoning capabilities. For instance, DEEPSEEK-R1’s performance improves further to 81.3% with the inclusion of few-shot CoT exemplars, demonstrating that carefully constructed demonstrations enhance reasoning quality and stability. This trend is particularly evident in the classical mechanics domain, where the few-shot accuracy rises from 62.5% to 84.8%.

4.2 PERFORMANCE IN DIFFERENT DOMAINS

Thermodynamics. Thermodynamics emerged as the most challenging domain, presenting unique difficulties even for top-performing models. Deepseek-R1’s 76.5% zero-shot accuracy in thermo, while respectable, represents a significant drop from its fundamental physics performance. Notably, few-shot prompting provided minimal improvements in this domain, suggesting that thermodynamics’ abstract, multi-step conceptual problems resist straightforward example-based learning.

270 **Fundamental Physics.** In fundamental physics, models achieved their strongest results, with
 271 Deepseek-R1 reaching 88.7% (zero-shot) and 93.0% (few-shot) accuracy. This superior performance
 272 aligns well with large language models' inherent strengths in pattern recognition and mathematical
 273 manipulation.

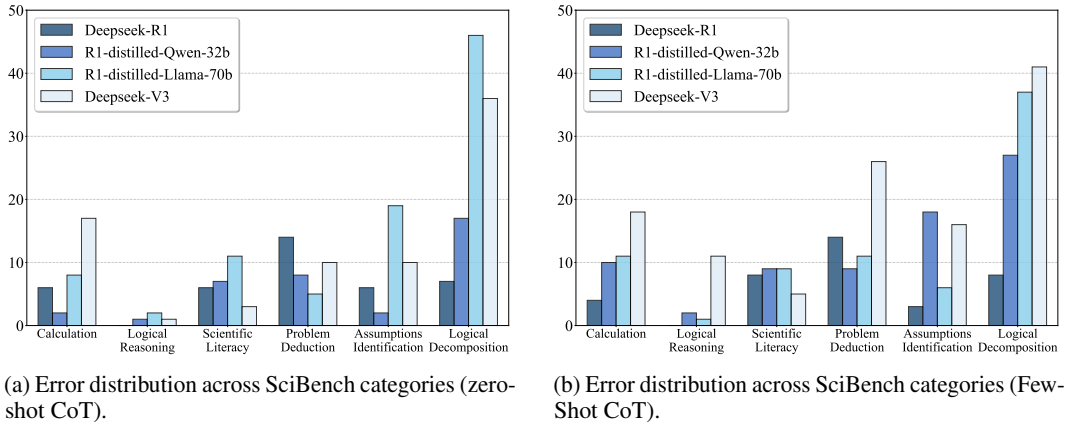
274 **Classical dynamics.** Classical dynamics showed the most dramatic response to few-shot learning
 275 techniques, offering encouraging insights about model adaptability. Deepseek-R1's performance in
 276 this domain jumped from 62.5% (zero-shot) to 84.8% (few-shot), indicating that classical mechanics'
 277 concrete, iterative problems are particularly amenable to contextual learning.

279 4.3 MODEL SIZE VS PERFORMANCE

281 In R1-distill models, The smaller R1-distill-Qwen-32B consistently outperforms its larger counterpart
 282 R1-distill-LLaMA-70B across most physics benchmarks, achieving superior scores in fundamental
 283 physics (76.1% vs. 64.8% zero-shot) and thermodynamics (74.5% vs. 55.4%). This result demon-
 284 strates that the Qwen architecture's superior symbolic processing capabilities more than compensate
 285 for its reduced parameter count. The performance advantage is particularly notable given the 32B
 286 model's significantly lower computational requirements.

287 The results also reveal that mid-sized distilled models rival much larger generalist models (e.g.,
 288 GPT-4), demonstrating that task-specific optimization outweighs pure scaling. Full-sized models
 289 like Deepseek-R1 still dominate in few-shot learning, suggesting that parameter count remains
 290 critical for in-context learning flexibility. Notably, R1-distill-Qwen-32B cuts match scores or even
 291 outperforms larger models like GPT-4 in throughput while preserving high-quality chain-of-thought
 292 reasoning. The performance advantage is particularly notable given the 32B model's significantly
 293 lower computational requirements. Therefore, distilled models strike an optimal balance between
 294 performance and resource utilization.

295 4.4 ERROR REDUCTION CATEGORIES



309 (a) Error distribution across SciBench categories (zero-
 310 shot CoT).

(b) Error distribution across SciBench categories (Few-
 311 Shot CoT).

312 Figure 2: Comparison of error distributions across different prompting methods, excluding near-zero
 313 categories

314 As Figures 2a and 2b show, We also analyze the performance improvement of Deepseek-R1 over
 315 Deepseek-V3, as well as few-shot over zero-shot prompting under R1, using error categories based
 316 on the essential scientific problem-solving skills defined in SciBench. (Note: SciBench includes 10
 317 error categories, but we exclude the zero and near-zero categories to focus on the major ones). The
 318 following categories have shown clear error reductions.

319 **Logical Decomposition.** Deepseek-R1 maintains exceptional performance with minimal degradation
 320 from 7 to 8 errors (14.3% increase), demonstrating robust logical decomposition capabilities that are
 321 largely independent of prompting strategy. R1-distilled-Llama-70b shows moderate improvement
 322 from 46 to 37 errors, representing a 19.6% improvement with few-shot examples. Deepseek-V3 ex-
 323 periences significant regression from 36 to 41 errors (13.9% increase), suggesting few-shot examples

324
325
326
327
328
329
330
331
332
333
334
335
336
337
338
339
340
341
342
343
344
345
346
347
348
349
350
351
352
353
354
355
356
357
358
359
360
361
362
363
364
365
366
367
368
369
370
371
372
373
374
375
376
377**Problem**

A food shipper pushes a wood crate of cabbage heads (total mass $m = 14$ kg) across a concrete floor with a constant horizontal force \vec{F} of magnitude 40 N. In a straight-line displacement of magnitude $d = 0.50$ m, the speed of the crate decreases from $v_0 = 0.60$ m/s to $v = 0.20$ m/s. Find the increase ΔE_{th} in the thermal energy of the crate and floor.

Step-by-Step Numeric Substitution**Step 1: Compute Work Done by the Push**

The work done by the applied force is:
 $W = F \cdot d = (40 \text{ N}) \cdot 0.5 \text{ m} = 20 \text{ J}$

Step 2: Compute ΔK

$$\Delta K = \frac{1}{2}m(v^2 - v_0^2)$$

Substituting the given values:

$$\Delta K = \frac{1}{2} \times 14 \text{ kg} \times ((0.20 \text{ m/s})^2 - (0.60 \text{ m/s})^2) = -2.2 \text{ J}$$

Step 3: Apply the Theorem

The work-energy theorem states:

$$W = \Delta K + \Delta E_{\text{th}}$$

Solving for the change in thermal energy:

$$\Delta E_{\text{th}} = W - \Delta K = 20 - (-2.2) = \boxed{22 \text{ J}}$$

Symbolic Derivation**Step 1: General Energy Relation**

The work-energy theorem, including thermal dissipation, states:

$$\Delta E_{\text{th}} = W - \Delta K$$

where:

$$W = F \cdot d$$

$$\Delta K = \frac{1}{2}m(v^2 - v_0^2)$$

Step 2: Symbolic Substitution

Substitute the expressions:

$$\Delta E_{\text{th}} = Fd - \frac{1}{2}m(v^2 - v_0^2)$$

Step 3: Numerical Calculation

Plug in the given values:

$$\Delta E_{\text{th}} = (40)(0.50) - \frac{1}{2}(14)(0.20^2 - 0.60^2) = 20 - 7(-0.32) = \boxed{22 \text{ J}}$$

Figure 3: Comparison of two solution strategies for finding the increase in thermal energy when a 14 kg crate is pushed 0.5 m by a 40 N force. **Left:** A step-by-step numeric approach, in which the work done by the push is calculated first, then the change in kinetic energy is determined, and finally the thermal energy increase is obtained by combining those results. **Right:** A symbolic approach, where a general expression for the thermal energy increase is derived in terms of work and kinetic energy change before the numerical values are inserted.

may introduce confusion for complex structural reasoning. R1-distilled-Qwen-32b shows the most dramatic decline from 17 to 27 errors (58.8% increase).

Calculation Skills. Few-shot prompting delivers mixed results across models. Deepseek-R1 achieves the best improvement, reducing errors from 6 to 4 (33.3% reduction), demonstrating enhanced arithmetic precision with worked examples. R1-distilled-Llama-70b shows modest improvement from 8 to 11 errors, while both Deepseek-V3 (17 to 18 errors) and R1-distilled-Qwen-32b (2 to 10 errors) exhibit performance degradation.

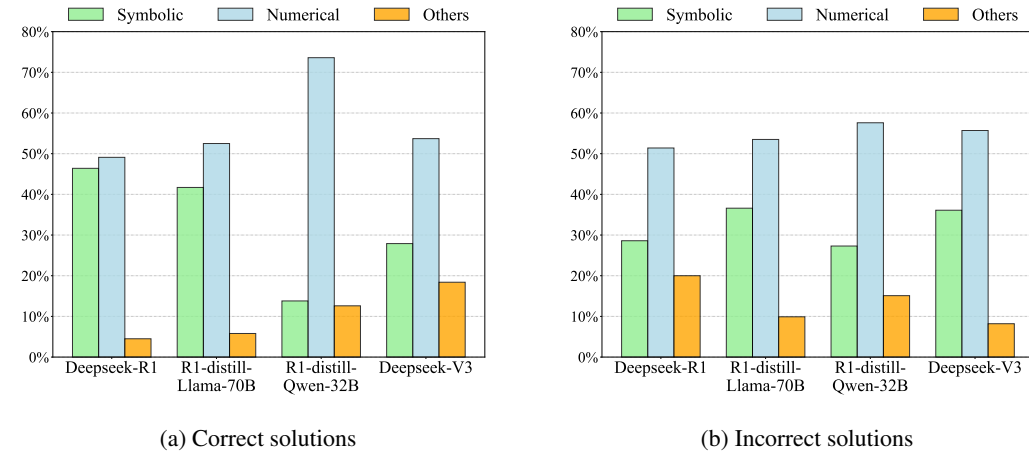
Assumption Identification. This category reveals the most pronounced few-shot benefits. Deepseek-R1 achieves a 50% error reduction from 6 to 3, demonstrating that exemplar-based prompting significantly enhances premise identification. R1-distilled-Llama-70b shows substantial improvement from 19 to 6 errors (68.4% reduction). However, both Deepseek-V3 (10 to 16 errors, 60% increase) and R1-distilled-Qwen-32b (2 to 18 errors, 800% increase) show concerning performance degradation, suggesting that few-shot examples may overwhelm these models’ assumption-detection mechanisms.

4.5 REASONING PATTERN

To further analyze the behavioral differences between models, we examine the chain-of-thought outputs of correct answers from selected models and identify two predominant reasoning patterns used when solving physics problems across the three datasets (See Figure 3) :

378 **Step-by-Step Numeric Substitution.** This approach represents a direct computational approach in
 379 which solvers immediately replace variables with given numerical values. This method progresses
 380 linearly through arithmetic operations at each stage, moving efficiently from known quantities to final
 381 answers.

382 **Symbolic Derivation.** This approach embodies a more theoretical approach that maintains variables
 383 in their symbolic form throughout initial problem-solving stages. Solvers using this method to firstly
 384 establish complete mathematical relationships between quantities, then substituting numerical values
 385 in the final computation steps.



404 Figure 4: Distribution of reasoning patterns in (a) correct and (b) incorrect solutions across different
 405 Deepseek model variants.

408 5 CONCLUSION

411 This study investigates the capabilities of advanced reasoning-focused large language models (LLMs)
 412 in solving complex physics problems, with a particular focus on the instruction-tuned model
 413 DEEPEEK-R1 and its distilled variants. Leveraging the SciBench benchmark, we systematically
 414 evaluate both zero-shot and few-shot Chain-of-Thought (CoT) prompting strategies.

415 Our results demonstrate that reasoning models consistently outperform general-purpose chat-based
 416 models across all datasets, even in zero-shot settings. Notably, DEEPEEK-R1 achieves substantial
 417 improvements in both accuracy and interpretability, generating step-by-step solutions that reflect a
 418 deep conceptual understanding and precise symbolic manipulation. While few-shot prompting further
 419 enhances performance, its impact is less critical for such high-performing reasoning models. This
 420 finding suggests that although prompting strategies can still improve reasoning models, they already
 421 achieve satisfactory accuracy without external methods. Furthermore, we identify a clear dichotomy
 422 in reasoning patterns between specialized and chat-oriented models: reasoning-specialized models
 423 often employ symbolic derivation—algebraically manipulating equations prior to numeric substitu-
 424 tion—particularly in correct solutions, while chat-oriented models, exemplified by Deepseek-V3,
 425 rely heavily on step-by-step numeric substitution, reflecting a more procedural and less abstract
 426 approach. This distinction provides critical insight into performance gaps observed in multi-step
 427 problems that demand abstract manipulation and structured reasoning. Collectively, these findings
 428 underscore the significance of symbolic reasoning as a key driver of robust performance, emphasizing
 429 the transformative potential of instruction-tuned reasoning models for physics education and complex
 430 scientific problem-solving tasks.

431 6 LIMITATIONS

432 Despite these promising findings, several limitations merit discussion. First, reasoning models
 433 such as DEEPSEEK-R1 incur substantial computational costs due to the verbose nature of CoT
 434 outputs. Compared to chat-oriented models, their
 435 step-by-step reasoning processes often result in
 436 significantly higher token counts—sometimes ex-
 437 ceeding 10,000 tokens for a single problem(See
 438 Table 3). This increases inference latency and
 439 places a heavy burden on both memory and processing resources, potentially limiting scalability in
 440 real-world deployments or low-resource environments Kaplan et al. (2020); Zhang et al. (2023). Also,
 441 our analysis is limited to unimodal, text-only problems and does not account for questions requiring
 442 diagrammatic interpretation, spatial reasoning, or numerical simulation. Extending these models to
 443 multimodal inputs remains a future direction. Alayrac et al. (2022); Driess et al. (2023).
 444

446 REPRODUCIBILITY STATEMENT

448 We have taken several measures to ensure the reproducibility of our results. All datasets used
 449 in our experiments are drawn from the publicly available SciBench benchmark, and we clearly
 450 describe our filtering criteria and dataset statistics in Section 1. The model configurations, inference
 451 parameters, and prompting strategies (zero-shot and few-shot CoT) are specified in Section 3 and
 452 Appendix A, including temperature settings, retry mechanisms, and exemplar selection. Detailed
 453 error categorization procedures and reasoning pattern analyses are described in Section 4.4 and
 454 Appendix B, with examples provided to illustrate our methodology. To further support reproducibility,
 455 we include prompt templates, evaluation scripts, and implementation details in the supplementary
 456 materials. Together, these resources allow independent researchers to replicate our experimental
 457 pipeline and validate the reported findings.

459 REFERENCES

461 Jean-Baptiste Alayrac, Jeff Donahue, Paul Luc, Antoine Miech, Serkan Cabi, Alec Radford, , et al.
 462 Flamingo: A visual language model for few-shot learning. *arXiv preprint arXiv:2204.14198*, 2022.
 463 URL <https://arxiv.org/abs/2204.14198>.

464 Tom B. Brown, Benjamin Mann, Nick Ryder, Melanie Subbiah, Jared Kaplan, Prafulla Dhari-
 465 wal, Arvind Neelakantan, Pranav Shyam, Girish Sastry, Amanda Askell, et al. Language
 466 models are few-shot learners. *Advances in Neural Information Processing Systems*, 33:1877–1901, 2020. URL <https://proceedings.neurips.cc/paper/2020/file/1457c0d6bfcb4967418bfb8ac142f64a-Paper.pdf>.

469 Andy Chen, Kevin Zhan, Sharan Saxena, Shashank Mani, Esin Durmus, and Xi Victoria Lin. Scibench:
 470 Evaluating scientific reasoning in large language models. *arXiv preprint arXiv:2311.16421*, 2023.
 471 URL <https://arxiv.org/abs/2311.16421>.

472 Hyung Won Chung, Le Hou, Shayne Longpre, Barret Zoph, Yi Tay, William Fedus, Xuezhi Wang,
 473 Mostafa Dehghani, Kelvin Guu, Maxwell Spisak, et al. Scaling instruction-finetuned language mod-
 474 els. *arXiv preprint arXiv:2210.11416*, 2022. URL <https://arxiv.org/abs/2210.11416>.

476 Danny Driess, Kira Munn, Iro Radosavovic, et al. Palm-e: An embodied multimodal language model.
 477 *arXiv preprint arXiv:2303.03378*, 2023. URL <https://arxiv.org/abs/2303.03378>.

478 Leo Gao, Stella Biderman, and Sid Black. Evaluating large language models trained on code. *arXiv
 479 preprint arXiv:2107.03374*, 2022. URL <https://arxiv.org/abs/2107.03374>.

481 Wenlong Huang, Shiyue Liu, Zhiruo Wu, Jiayi Lei, Deyao Chen, Shixiang Chen, Yunfan Zhang, and
 482 Maosong Sun. Tool-augmented language models. *arXiv preprint arXiv:2305.02434*, 2023. URL
 483 <https://arxiv.org/abs/2305.02434>.

484 Jared Kaplan, Sam McCandlish, Tom Henighan, Tom Brown, Benjamin Chess, Rewon Child, Scott
 485 Gray, Alec Radford, Jeffrey Wu, and Dario Amodei. Scaling laws for neural language models.
 486 *arXiv preprint arXiv:2001.08361*, 2020. URL <https://arxiv.org/abs/2001.08361>.

Table 3: Average output tokens per model on the same question set.

Model	Avg. Output Tokens
Deepseek-R1	14,698
R1-distill (LLaMA-70B)	7,688
R1-distill (Qwen-32B)	8,355
Deepseek-V3	4,035

486 Takeshi Kojima, Shixiang Shane Gu, Machel Reid, Yutaka Matsuo, and Yusuke Iwasawa. Large
 487 language models are zero-shot reasoners. *Advances in Neural Information Processing Systems*, 35:
 488 22140–22155, 2022. URL <https://openreview.net/forum?id=0XgTvgQLjJ>.

489

490 Patrick Lewis, Ethan Perez, Aleksandra Piktus, Fabio Petroni, Vladimir Karpukhin, Naman Goyal, Ilia
 491 Kulikov, Heinrich Mikenina, Wen-tau Yih, Tim Rocktäschel, et al. Retrieval-augmented generation
 492 for knowledge-intensive nlp tasks. In *Advances in Neural Information Processing Systems*,
 493 volume 33, pp. 9459–9474, 2020. URL <https://proceedings.neurips.cc/paper/2020/hash/6b493230205f780e1bc26945df7481e5-Abstract.html>.

494

495 Yifei Li, Yuntao Bai, Jeffrey Wu, Barret Zoph, and Denny Zhou. Instruction-tuning in reasoning
 496 tasks. *arXiv preprint arXiv:2403.01456*, 2024. URL <https://arxiv.org/abs/2403.01456>.

497

498 Hanxiao Liu, Mohammad Saleh, Ian Goodfellow, Noam Shazeer, William Fedus, Colin Raffel, Adam
 499 Roberts, Barret Zoph, Christian Szegedy, and Lukasz Kaiser. Program-aided language models.
 500 *arXiv preprint arXiv:2304.02988*, 2023. URL <https://arxiv.org/abs/2304.02988>.

501

502 Aman Madaan, Xiang Lin, Ni Ke, Xinyu Liu, Amir Yazdanbakhsh, Rishabh Singh, Preetam Jain,
 503 Trishul Chilimbi, Mohit Iyyer, and Graham Neubig. Language models can solve computer tasks.
 504 *arXiv preprint arXiv:2306.02775*, 2023. URL <https://arxiv.org/abs/2306.02775>.

505

506 Maxwell Nye, Rik Koncel-Kedziorski, Oyvind Tafjord, Antoine Bosselut, and Ashish Sabharwal.
 507 Self-verification for large language models. *arXiv preprint arXiv:2401.04867*, 2024. URL
 508 <https://arxiv.org/abs/2401.04867>.

509

510 OpenAI. Gpt-4 technical report. <https://arxiv.org/abs/2303.08774>, 2023. arXiv preprint
 511 [arXiv:2303.08774](https://arxiv.org/abs/2303.08774).

512

513 Long Ouyang, Jeffrey Wu, Xu Jiang, Diogo Almeida, Carroll Wainwright, Pamela Mishkin, Chong
 514 Zhang, Sandhini Agarwal, Katarina Slama, Alex Ray, et al. Training language models to follow
 515 instructions with human feedback. *Advances in Neural Information Processing Systems*, 35:
 516 27730–27744, 2022. URL <https://openai.com/research/instruction-following>.

517

518 Shaden Smith, Austin Prager, Denis Kocetkov, Dhruv Narayanan, Hugo Touvron, Thomas Wolf,
 519 Teven Le Scao, and Deepak Narayanan. Reasoning curricula for language models. *arXiv preprint
 520 arXiv:2308.12345*, 2023. URL <https://arxiv.org/abs/2308.12345>.

521

522 Rohan Taori, Ishaan Gulati, Tianyi Zhang, Yann Dubois, Xuechen Dave, et al. Stanford alpaca: An
 523 instruction-following llama model. https://github.com/tatsu-lab/stanford_alpaca,
 524 2023. Online, accessed April 2024.

525

526 Jason Wei, Xuezhi Wang, Dale Schuurmans, Maarten Bosma, Brian Ichter, Fei Xia,
 527 Ed Chi, Quoc V. Le, and Denny Zhou. Chain-of-thought prompting elicits reasoning in
 528 large language models. *Advances in Neural Information Processing Systems*, 35:24824–
 529 24837, 2022. URL https://proceedings.neurips.cc/paper_files/paper/2022/file/9d5609613524a45b2ba5e6e9a6e4ba68-Paper-Conference.pdf.

530

531 Shixiang Shane Zhang, Jiaming Yang, Diyi Yang, Weijia Chen, Xiang Lin, Maosong Sun, and
 532 Denny Zhou. Language model cascades. *arXiv preprint arXiv:2303.08774*, 2023. URL <https://arxiv.org/abs/2303.08774>.

533

534 Yuxuan Zheng, Yichong Zhu, Xiang Lin, Barret Zoph, Kelvin Guu, Jason Wei, Peter J. Liu, and
 535 Denny Zhou. Prompt engineering for advanced language models. *arXiv preprint arXiv:2402.06789*,
 536 2024. URL <https://arxiv.org/abs/2402.06789>.

537

538

539

540
541

A EXPERIMENT DETAILS

542
543

A.1 MODEL INVOCATION AND ROBUSTNESS

544
545

We wrap the OpenAI chat API call in a `Caller` class that: Uses a deterministic temperature ($T = 10^{-30}$). Retries up to a large patience count, with optional sleep between retries. Checks for non-empty responses before returning. Logs API errors to `stderr` and continues retrying.

546
547

A.2 OUTPUT PARSING AND EVALUATION

548
549

The raw model output is post-processed to extract the numeric answer: Strip LaTeX boxing and other text. Normalize “not”-style units via `remove_not/cal_not`. Compare to ground-truth using `math.isclose` with 5% relative tolerance. Per-problem correctness is logged, and final accuracy is reported over the entire dataset.

550
551

A.3 API USAGE

552
553

We instantiate the OpenAI client with the user’s API key and OpenRouter base URL. We wrap each call in a retry loop with exponential backoff—initial sleep of 2 s doubling each retry—up to a maximum number of attempts. Before accepting a response, we validate that `response.choices` exists and contains non-empty `message.content`. Errors (network, rate limits, empty responses) are caught, logged, and trigger the backoff logic. This pattern ensures robust, deterministic interaction with OpenRouter while preserving per-problem logging and progress reporting.

554
555

A.4 PROMPT CONSTRUCTION

556
557

To maintain the completeness and consistency of the experiment, the prompt construction follows the same format as the experimental setup used in SciBench Chen et al. (2023). For few-shot CoT evaluation, the prompt begins with a system message that defines the assistant’s role (e.g., a helpful and accurate physics tutor), followed by several solved example problems. Each example includes a user query presenting the problem statement and an assistant response that provides both the step-by-step reasoning and the final boxed answer with units. The test problem is appended afterward without a solution. For zero-shot and zero-shot CoT settings, no examples are provided. Instead, the prompt contains only the system message and a single user query for the test problem. In the zero-shot CoT setting, we apply a two-stage prompting strategy: the first prompt elicits intermediate reasoning (“Let’s think step by step”), and the second prompt feeds back this reasoning to request a final answer. All prompts include explicit unit information by appending “The unit of the answer is `<unit>`” to the problem text to reduce ambiguity and encourage unit-aware predictions.

558
559

A.5 HUMAN EVALUATION

560
561

For reasoning pattern analysis, we involve human in the loop review to check the chain of thought and solutions of the answers, then identify the specific patterns into several categories:

562
563

1. Problem Restatement
2. Formula Selection & Symbolic Derivation
3. Step-by-Step Numeric Substitution
4. Multi-Path or Case Enumeration
5. Forward vs. Backward Reasoning
6. Self-Check & Validation

564
565

Then construct specific prompts for LLMs to identify the pattern of each answer.

566
567

B TOKEN LEVEL ANALYSIS

568
569

We also perform token level analysis in the experiment. To quantify the internal certainty and decisiveness of reasoning models during CoT generation, we propose two token-level metrics: *average token confidence* and *average token gap*. These statistics offer fine-grained insight into the reliability of the model’s reasoning process.

594 B.1 AVERAGE TOKEN CONFIDENCE
595596 Let the model generate a reasoning chain of N tokens. The token confidence is defined by:
597

598
$$\ell_i = \log P(t_i | t_{<i}), \quad p_i = \exp(\ell_i)$$

599
$$600 \text{avg_confidence} = \frac{1}{N} \sum_{i=1}^N p_i \quad (\times 100\%).$$

601

602 A higher average confidence reflects the model’s self-assessed certainty in generating each step of its
603 reasoning chain.604 B.2 AVERAGE TOKEN GAP
605606 To assess decisiveness at each token step, we define the token gap as the difference between the top-1
607 and top-2 token probabilities:
608

609
$$610 g_i = \ell_i^{(1)} - \ell_i^{(2)}, \quad \text{avg_token_gap} = \frac{1}{N} \sum_{i=1}^N g_i$$

611

612 C LLM USAGE
613614 The authors would like to acknowledge the use of OpenAI’s GPT-4.5 OpenAI (2023) for grammar
615 polishing and language enhancement in this paper. The AI tool was used solely for improving the
616 clarity and readability of the text, while all technical content, ideas, and conclusions remain the
617 authors’ own. We appreciate the advancements in AI-assisted writing tools that help researchers
618 communicate their work more effectively.
619620
621
622
623
624
625
626
627
628
629
630
631
632
633
634
635
636
637
638
639
640
641
642
643
644
645
646
647

648
649
650
651
652
653
654
655
656
657
658
659
660
661
662
663
664
665
666
667
668
669
670
671
672
673
674
675
676
677
678
679
680
681
682
683
684
685
686
687
688
689
690
691
692
693
694
695
696
697
698
699
700
701

Prompt Template for Reasoning Pattern Analysis

Review the problem statement, the reference solution, and the model’s chain-of-thought. Identify which one of the following high-level reasoning patterns the model employs, then output only the category number or name:

Problem Restatement & Known-Quantity Definition

- The model starts by paraphrasing the question and listing all given variables with their symbols.

Formula Selection & Symbolic Derivation

- The model names the governing law or equation, performs any algebraic rearrangements symbolically, then substitutes numbers.

Step-by-Step Numeric Substitution

- The model breaks down each formula into small steps, plugs in values, computes intermediate results, and carries them forward.

Multi-Path or Case Enumeration

- The model either runs two or more equivalent solution methods in parallel or enumerates multiple sign/geometric cases, then picks the valid result.

Forward vs. Backward Reasoning

- *Forward*: from known data to answer step by step.
- *Backward*: start with the final condition/equation, then solve backward for the unknown.

Self-Check & Validation

- After key steps, the model pauses to sanity-check units or compare parallel-path results before proceeding.

Figure 5: Prompt for analyzing reasoning patterns

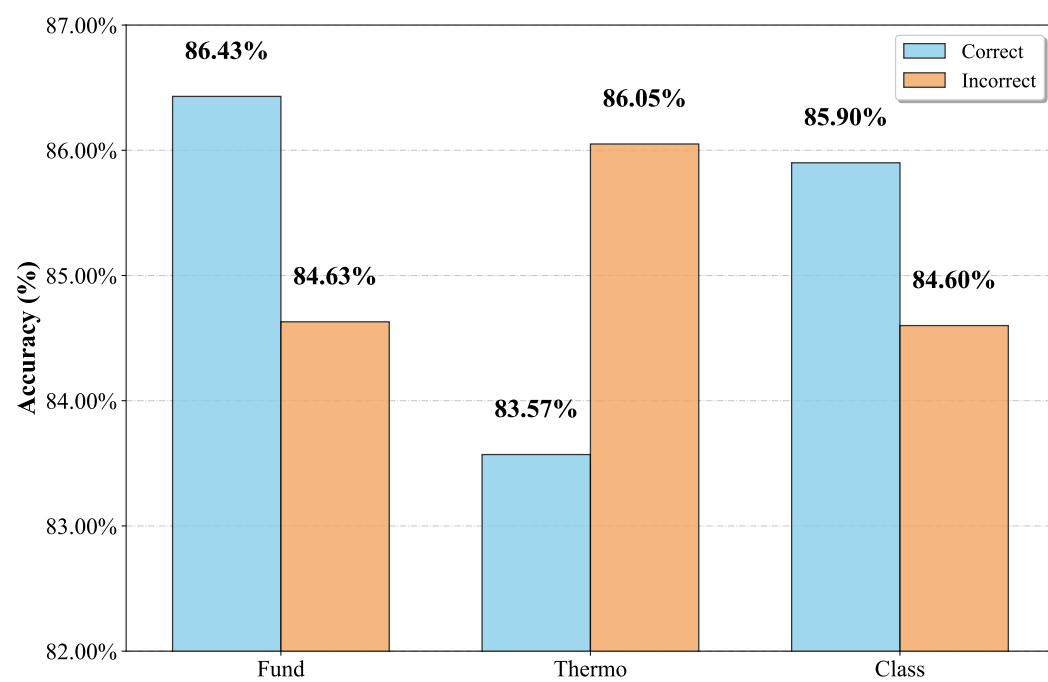


Figure 6: Average token confidence for correct vs. incorrect answers.

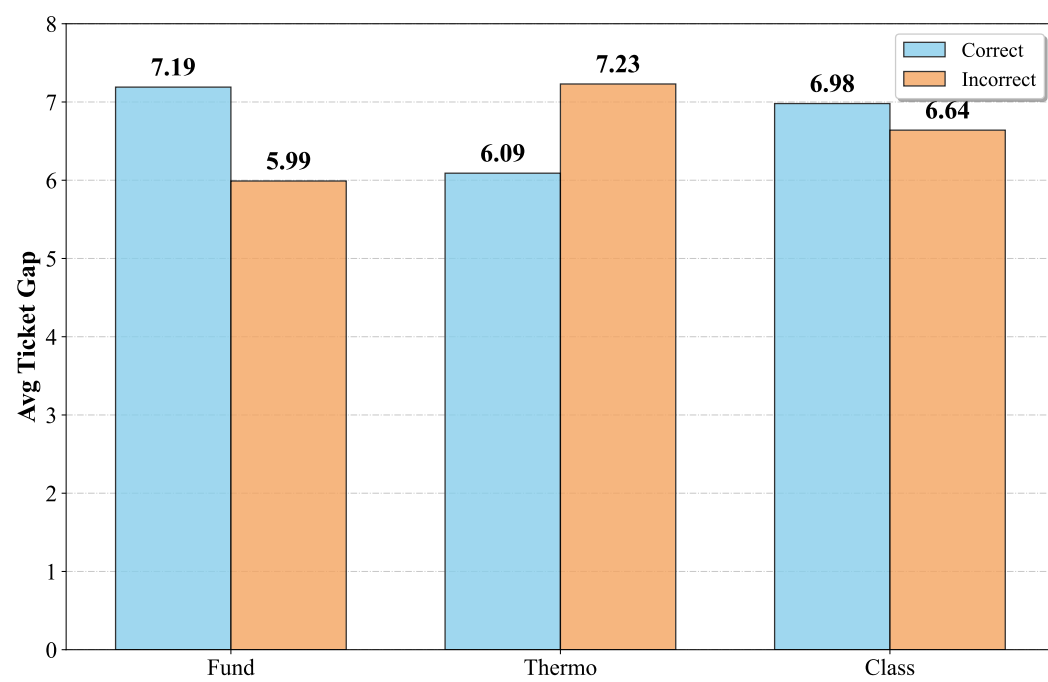


Figure 7: Average token gap for correct vs. incorrect answers.